Check for updates

Chemistry–A European Journal
Research Article
doi.org/10.1002/chem.202301669
Chemistry Europe
European Chemical Societies Publishing
www.chemeurj.org

The Role of Inverted Ligand Field in the Electronic Structure and Reactivity of Octahedral Formal Platinum (IV) Complexes**

Andrea Ienco,[a] Francesco Ruffo,[b] and Gabriele Manca*[a]

Platinum complexes are ubiquitous in chemistry and largely used as catalysts or as precursors in drug chemistry, thus a deep knowledge of their electronic properties may help in planning new synthetic strategies or exploring new potential applications. Herein, the electronic structure of many octahedral platinum complexes is drastically revised especially when they feature electronegative elements such as halogens and chalcogens. The investigation revealed that in most cases the five d platinum orbitals are invariably full, thus the empty antibonding orbitals, usually localized on the metal, are mainly centered on the ligands, suggesting a questionable assignment of formal oxidation state IV. The analysis supports the occurrence of the inverted ligand field theory in all cases with the only exceptions of the Pt–F and Pt–O bonding. The trends for the molecular complexes are mirrored also by the density of states plots of extended structures featuring octahedral platinum moieties in association with chalcogens atoms. Finally, the oxidative addition of a Se–Cl linkage to a square platinum complex to achieve an octahedral moiety has been revised in the framework of the inverted ligand field.

Introduction

The classical accepted view of the metal-ligand interactions in a transition metal complex is based on the assumption that the ligand-based combinations are filled and at lower energy than the involved metal orbitals (ligand field theory).[1–3] This description provides an immediate picture of the electronic distribution in most transition metal complexes. For the late transition metals, the energy of the d orbitals may be lower than the ligand ones, as it occurs in some square planar "d^8" complexes where the b_{1g} ligands combination lies in energy above the interacting metal d_{x2-y2} orbital.[4] As shown at the right side of Scheme 1, the resulting σ bonding orbital is mainly centered on the metal while the antibonding σ* one (usually the LUMO) features a stronger contribution from the ligands with an electron population towards the metal center. This bonding picture in square planar complexes allowed the introduction of the concept of Inverted Ligand Field (ILF).[1,5]

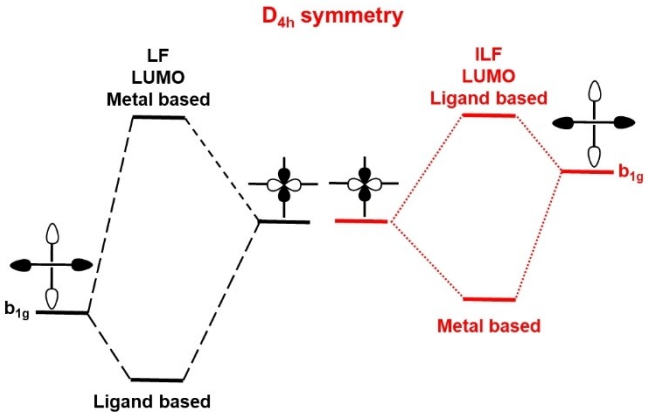

Scheme 1. Evolution of the electronic structure for σ bonding on increasing the energy of the b_{1g} ligands' combination for a square planar transition metal complex.

The ILF theory, nowadays well supported by experimental data and calculations,[1,5–16] provides a critical review of the high formal oxidation state in 11th group metals suggesting that most of the d^8 Cu(III) and Au(III) square planar complexes could be better considered as d^{10} Cu(I) and Au(I) ones with electronic holes on the ligands. This new bond description allows a better knowledge of the reactivity of these systems, not always easily to be rationalized. Theoretical and spectroscopic investigations on silver, especially Ag(II), based complexes and materials have highlighted electronic structures approaching the ILF description with covalent of M-ligand bonding.[11] ESR and optical investigation on silver(II) impurities in crystalline structures with halides highlighted the strong covalency of the bond and a metal configuration close to d^{10}.[17,18] Similar results were pointed out also for other crystal structures of silver oxides with the presence of electronic holes on oxygen atoms.[19,20] Exper-

[a] Dr. A. Ienco, Dr. G. Manca
Istituto di Chimica dei Composti Organometallici
Consiglio Nazionale delle Ricerche
Via Madonna del Piano 10, 50019 Sesto Fiorentino, Firenze (Italy)
E-mail: gabriele.manca@cnr.it
[b] Prof. F. Ruffo
Dipartimento di Scienze Chimiche
Università degli Studi di Napoli Federico II
Complesso Universitario di Monte Sant'Angelo, via Cintia 21, Napoli (Italy)

[**] A previous version of this manuscript has been deposited on a preprint server (https://doi.org/10.26434/chemrxiv-2023-5szvm).

Supporting information for this article is available on the WWW under https://doi.org/10.1002/chem.202301669

© 2023 The Authors. Chemistry - A European Journal published by Wiley-VCH GmbH. This is an open access article under the terms of the Creative Commons Attribution License, which permits use, distribution and reproduction in any medium, provided the original work is properly cited.

© 2023 The Authors. Chemistry - A European Journal published by Wiley-VCH GmbH

imental validation of the ILF is available for some d^8 Ag(III) complexes such as in $[AgF_4]^-$ anion, where, although silver is coordinated to four fluoride ligands, the spectroscopic experiments highlight a large covalency of Ag–F bonds and an electronic distribution far from the generally proposed Ag-(III)$(F^-)^4$ one.[21]

Scheme 1 shows how the LUMO becomes the key orbital for discriminating between a LF and a ILF descriptions. A metal contribution to the LUMO greater than 60% allows a more suitable description of the σ-bonding within the classic LF theory with the bonding electrons more localized on the ligands. Otherwise, when the contribution of the metal to the LUMO is small (less than 40%) the ILF becomes operative, and the σ M–L bonding could be better described as covalent with the electrons more polarized toward the metal rather than the ligands. Obviously, a wide spectrum of intermediate situations of σ covalency is possible in the contribution range between 40 and 60% with the maximum of covalent bond for 50% contribution.[1,5,7]

Herein, we explore the chance that ILF could be active also in a coordination geometry alternative to the square planar, namely the octahedral one, and for platinum in formal oxidation state IV. In a classical viewpoint, the bonding in octahedral complexes could be described as six electron pairs donations from the six populated ligands into six empty suitable metal orbitals (one s, three p and two d in the e_g set namely d_{x2-y2} and d_{z2}) assuming the ligands at lower energy than the metal d orbitals. Thus, in an octahedral arrangement, as for instance in $[PtX_6]^{2-}$, the LUMO and the LUMO + 1 should have a σ* feature according to the traditional rules and are mainly localized on the metal center. Conversely, the σ bonding combinations are very stabilized in energy, fully populated and with a great contribution from the ligands. Scheme 2 compares the LF and ILF in a O_h symmetry. In contrast to the square planar cases, the two e_g orbitals, namely d_{x2-y2} and d_{z2}, could be involved in ILF.

Herein, we provide a revision of the electronic structure of the octahedral platinum complexes in formal oxidation state IV with one or more metal center(s) surrounded by six halide or chalcogenide ions, among the most electronegative representatives of the periodic table in the perspective of Inverted Ligand Field. This helps to rationalize in a new way the reactivity of octahedral platinum complexes that are employed as intermediates in catalysis[22–25] and/or as drugs in medicinal chemistry.[26–33] A case study of application of the ILF to the platinum(IV) reactivity has also been discussed.

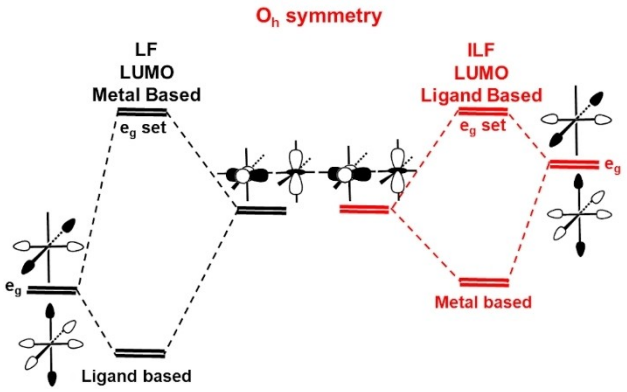

Scheme 2. Evolution of the electronic structure for σ bonding on increasing the energy of the e_g ligands' combination for an octahedral transition metal complex.

Results and Discussion

Chemical bonding in dianionic octahedral species $[PtX_6]^{2-}$ with X = halogen

Octahedral platinum(IV) complexes featuring six equivalent halide ions in the metal coordination sphere are well known, more than 200 X-ray structures containing halides ranging from iodide up to fluoride were found on the Cambridge Crystallographic Database.[34] The first step of the computational analysis was the optimization of the isolated anionic molecular complexes sharing the general formula $[PtX_6]^{2-}$ with X = halogen atom at BP86-DFT level of theory[35] with the inclusion of the dispersion forces effects. Zero-Order Regular Approximation (ZORA)[36] for platinum and iodine have been used as implemented in ORCA 5.0 software (more details of Computational Methodology are shown in Supporting Information).[37] A detailed analysis of the electronic structure was carried out with particular attention to the metal and ligand contributions to the lowest unoccupied molecular orbital (LUMO) and the closer MOs, taken as a primary diagnostic tool. Figure 1 shows the plots of the antibonding LUMO and the LUMO + 1 of the dianionic species $[PtI_6]^{2-}$ and the corresponding bonding counterparts at very low energy, being the HOMO-18 and HOMO-19, together with the relative metal/ligands contribution.

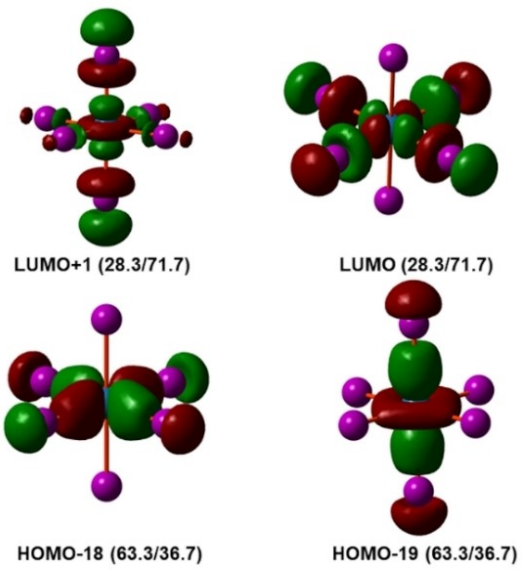

Figure 1. LUMO and LUMO + 1 σ*-bonding and occupied molecular orbitals with a large contribution from d platinum orbitals. The percentages of the metal vs. ligands contribution are reported in round brackets.

© 2023 The Authors. Chemistry - A European Journal published by Wiley-VCH GmbH

15213765, 2023, 59, Downloaded from https://chemistry-europe.onlinelibrary.wiley.com/doi/10.1002/chem.202301669 by CNR Group, Wiley Online Library on [13/11/2023]. See the Terms and Conditions (https://onlinelibrary.wiley.com/terms-and-conditions) on Wiley Online Library for rules of use; OA articles are governed by the applicable Creative Commons License

The LUMO and the LUMO+1 have a σ* antibonding character with a contribution from the six ligands larger than 70% *ca.* and less the 30% from platinum. The five d orbitals are filled and localized at low energy (d_{xz}, d_{yz} and d_{xy}) with the d_{x2-y2} and d_{z2} closing the series, being the HOMO-18 and HOMO-19, respectively. The latter two are mainly involved in the σ bonding counterparts of the LUMO and LUMO+1 orbital being the metal contribution of 63% and only 37% from the ligands. Such an electronic distribution suggests the occurrence of the ILF. By increasing the electronegativity of the halide up to chloride, the relative order of the orbitals shown in Figure 1 remains unaltered, although the contributions from the metal or the group of the ligands vary in a consistent trend. While for the bromine case the ILF occurrence has been also ascertained, chlorine represents a limiting case being the platinum contribution to LUMO and LUMO+1 close to 40%. In all cases, the Inverted Ligand Field could be reasonably invoked rather than the classic Ligand Field, confirming the d^{10} metal configuration with a strong covalency of the Pt-halide bonds also in combination with electronegative elements such as chlorine. The situation drastically changes when the platinum is combined with fluoride ligands, the most electronegative element of the Periodic table. In this regard, the LUMO and LUMO+1 feature a strong metal contribution (60% *ca.*) while the corresponding bonding combinations are mainly localized on the fluoride ligands, approaching the classic Ligand Field description. By fitting the Pauling electronegativity[38] of the halide vs. the contribution of the metal to the lower empty molecular orbitals (LUMO and LUMO+1), a linear interpolation, shown in Figure 2, has been obtained with a R value very close to one, suggesting a linear dependence of the ILF occurrence on the electronegativity of the halides. The larger is the halide electronegativity and the more stabilized become the ligands' combinations, thus less probable is the occurrence of the ILF. Satisfactorily linear fitting could be obtained also by using other kind of electronegativity values.[39]

To provide further validation of the proposed model, we focused our attention on the electronic structure of the trinuclear compound $[Pt_3Br_{12}]^{2-}$ featuring platinum in both octahedral and square planar coordination environments.[40] As shown in the upper part of Figure 3, two bromine of each of the lateral octahedral units bridge the central metal atom, which attains a square planar arrangement. $[Pt_3Br_{12}]^{2-}$ is traditionally described as a mixed valence compound with a formal oxidation state IV for the platinum atoms in octahedral environment and II for the central one. The optimized structure nicely reproduces the crystallographic one except for an overestimation of the Pt–Br distances no larger than 0.05 Å (the average experimental values are reported in brackets) and a somewhat distortion of the structure from the planarity.

All the lowest unoccupied molecular orbitals, shown in the lower part of Figure 3, are mainly localized on the bromide ligands with a lower contribution from the metal. LUMO and the LUMO+1 feature the *in-phase* and *out-of-phase* combinations of the metal d_{x2-y2} while LUMO+2 and LUMO+3 are the corresponding combinations of the Pt d_{z2} orbitals. The metal contributions remain lower than 37%. LUMO+4 is otherwise mainly localized on the central square planar complex with a 42.7% contribution from d_{x2-y2} metal center, which should be empty in a d^8 configuration. Thus, the electronic structure analysis raises many doubts on the formal oxidation state IV of the octahedral platinum centers highlighting a somewhat degree of covalence of the Pt(square planar)-Br linkages.

Chemical bonding in dianionic octahedral species featuring six chalcogenides

Once ascertained that the only exception to the ILF description for the octahedral platinum complexes with six halides is $[PtF_6]^{2-}$, the complexes featuring six chalcogen atoms have been investigated. The occurrence of the Inverted Ligand Field in gold compounds associated with chalcogens has been already pointed out some years ago in the unique gold mineral calaverite, $AuTe_2$.[41] The mineral exhibits a CdI_2-type structure with the Te atoms between triangles of gold with the presence of direct Te–Te interactions (3.20 Å).[41] The electronic structure of such a crystal has been largely debated since, according to the classic rules, a formal oxidation state II could be assigned to

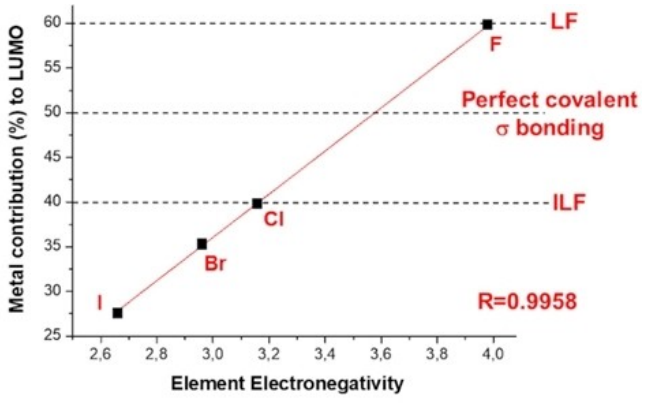

Figure 2. Linear dependence of the platinum contribution (%) to the LUMO and LUMO+1 by the electronegativity[38] of coordinated halides.

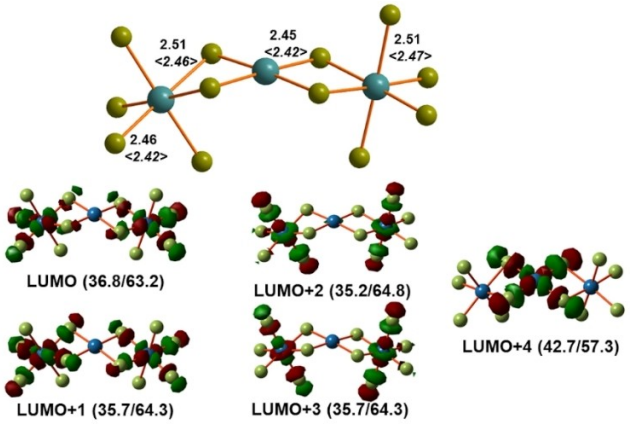

Figure 3. Upper part: Optimized structure of $[Pt_3Br_{12}]^{2-}$ (the experimental values are reported in brackets). Lower part: lowest unoccupied orbitals with the corresponding metal/ligands contribution in round brackets.

© 2023 The Authors. Chemistry - A European Journal published by Wiley-VCH GmbH

15213765, 2023, 59, Downloaded from https://chemistry-europe.onlinelibrary.wiley.com/doi/10.1002/chem.202301669 by CNR Group, Wiley Online Library on [13/11/2023]. See the Terms and Conditions (https://onlinelibrary.wiley.com/terms-and-conditions) on Wiley Online Library for rules of use; OA articles are governed by the applicable Creative Commons License

the gold centers The unusual paramagnetic d^9 gold configuration has been hypothesized to evolve through a spontaneous charge disproportionation to d^{10} and d^8 configurations. A recent spectroscopic and computational analysis solved the dilemma supporting a d^{10} configuration for all the gold centers with electronic holes localized on the ligands. Such a description of the electronic distribution of the calaverite perfectly fits with the ILF one. Conversely to the case of gold, platinum octahedral isolated complexes featuring ligands formed by only chalcogen atoms are known for the sulfur and selenium species. The first step of the computational investigation of the platinum chalcogenides started with the analysis of the electronic structure of the dianionic octahedral species of $[Pt(Se_4)_3]^{2-}$ and $[Pt(S_5)_3]^{2-}$ featuring the metal center surrounded by three η^2–Se_4^{2-}[42] or S_5^{2-}[43] ligands. The optimized structures of the selenium and sulfur platinum complexes are shown in Figure 4.

The optimized structures well reproduce the X-ray ones except for an 0.03 Å overestimation of the Pt-chalcogen distances In particular, in the $[Pt(Se_4)_3]^{2-}$ case the experimental Pt–Se distances are in 2.48–2.51 Å range while for $[Pt(S_5)_3]^{2-}$ are between 2.38 and 2.42 Å. Similarly, to the halide cases, the electronic structure of the compounds highlighted the complete occupancy of the five d orbitals of platinum with a small metal contribution to the lowest unoccupied orbitals, once again in contrast with the fundaments of the Ligand Field theory. In particular, Figure 5 shows the LUMO and LUMO + 1 of the $[Pt(Se_4)_3]^{2-}$ complex together with the $d_{x2\text{-}y2}$ and d_{z2}

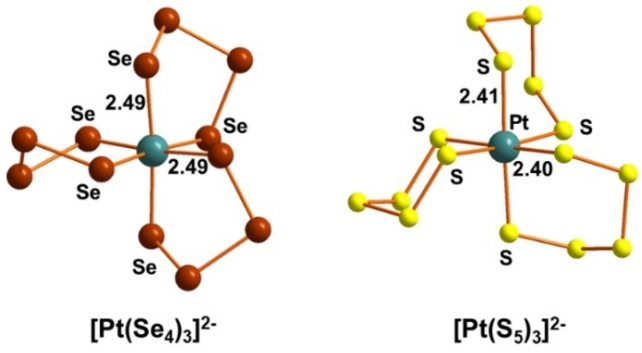

Figure 4. Optimized structure of $[Pt(Se_4)_3]^{2-}$ and $[Pt(S_5)_3]^{2-}$ octahedral platinum complexes.

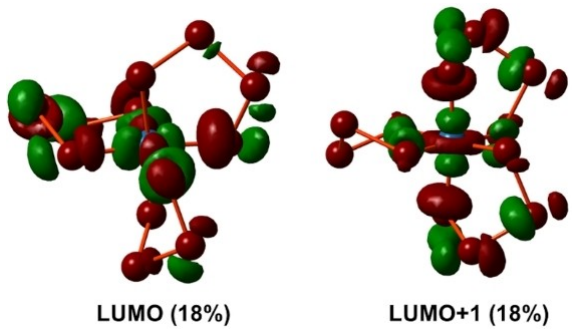

Figure 5. Lowest unoccupied molecular orbitals LUMO and LUMO + 1 of $[Pt(Se_4)_3]^{2-}$ complex together with the metal d orbital contribution.

platinum contribution, not larger than 18 %. A similar situation occurs in the sulfur complex $[Pt(S_5)_3]^{2-}$ although the percentage contribution from the platinum in LUMO and LUMO + 1 slightly increases up to 23 %, always remaining in the ILF framework.

For the sake of comparison, the electronic structure of an octahedral platinum complex featuring six oxygen-based ligands has been examined. In the absence of complexes featuring ligands only formed by oxygen atoms, the dianionic species $[Pt(CF_3COO)_6]^{2-}$ with six trifluoroacetate moieties has been chosen.[44] Conversely to the precedent cases with selenium and sulfur, the contribution of platinum to the lowest unoccupied orbitals LUMO and LUMO + 1(shown in Figure S1) becomes as large as 50.4 %, suggesting a pure covalent Pt–O bonding with an electronic situation halfway between the classic LF and the ILF description. Thus, similarly to the halogen cases, the more electronegative is the involved chalcogen, the most stabilized become the ligands' combinations and the more covalent becomes the bond or, in the limiting cases, the LF.

Understanding the electronic structure of the isolated octahedral platinum complexes with chalcogen ligands acquires particular importance also in view of the great interest of material science toward the 10th group transition metal dichalcogenides, TMDs. These materials feature a layered structure with the metal centers in an octahedral environment and each chalcogen bridging three different platinum centers. The closeness in energy between the metal d orbitals and the valence p ones of the chalcogen is particularly intriguing since, by changing the nature of the chalcogen element, a drastic variation of the electronic properties of the material may occur. For example, $PtTe_2$ behaves as a metal, $PtSe_2$ is a semimetal while PtS_2 is a semiconductor. Pumera et al.[45] pointed out how the electronic properties as well as the photocatalytic properties of the 10th group TMDs are particularly affected by the nature of the chalcogen. XPS experiments revealed no reasonable peaks for Pt(IV) in $PtTe_2$ and PtS_2 suggesting a 0 formal metal oxidation state for the tellurium species and a prevalence of Pt(II) in PtS_2. In this regard, the ILF model could be reasonable invoked in such solid-state structures and the obtained results perfectly agree with those obtained by Jobic et al.,[46] who considered improbable the assignment of a formal oxidation state IV to platinum when associated to tellurium. For solid state systems, the bottom part of the conduction band could provide useful hints on the electronic structure, especially from the analysis of the metal contribution analogously to the LUMO in the molecular systems. The quantitative contribution was estimated based on the Density of State plots of the $PtTe_2$, $PtSe_2$, PtS_2 and PtO_2, similarly to those obtained by Jobic et al.[46] and shown in Figure S2. The obtained trends perfectly agree with the ones obtained on molecular systems, the most electronegative is the chalcogen and the larger is the metal contribution to the bottom part of the conduction band, thus the more appropriate description becomes a covalent one. This is evident in the case of the oxygen atom where the metal and oxygen contributions are 58 and 42 %, respectively.

© 2023 The Authors. Chemistry - A European Journal published by Wiley-VCH GmbH

15213765, 2023, 59, Downloaded from https://chemistry-europe.onlinelibrary.wiley.com/doi/10.1002/chem.202301669 by CNR Group, Wiley Online Library on [13/11/2023]. See the Terms and Conditions (https://onlinelibrary.wiley.com/terms-and-conditions) on Wiley Online Library for rules of use; OA articles are governed by the applicable Creative Commons License

15213765, 2023, 59, Downloaded from https://chemistry-europe.onlinelibrary.wiley.com/doi/10.1002/chem.202301669 by CNR Group, Wiley Online Library on [13/11/2023]. See the Terms and Conditions (https://onlinelibrary.wiley.com/terms-and-conditions) on Wiley Online Library for rules of use; OA articles are governed by the applicable Creative Commons License

Inverted ligand field in a reactivity: A case study

Having the analyses highlighted how the assignment of the formal oxidation state IV is somewhat inappropriate for the octahedral platinum complexes, we reconsidered an "oxidative addition" reaction to a Pt(II) complex In particular, the activation of the chalcogen/halogen Se–Cl bonding of PhSe–Cl by square platinum complex [Pt{CH(CO_2Me)(CN)}$_2$(Bu_2-bipy)] (Bu_2-bipy = 4,4′-di-t-butyl-2,2′-bipyridine), shown in Scheme 3, has been investigated providing the octahedral "Pt(IV)" species [Pt{CH-(CO_2Me)(CN)}$_2$(Bu_2-bipy)(SePh)(Cl)].[47] A simplified model of the real complex using the bipyridine moiety in place of the t-butyl one has been used for the calculations.

As expected, the occurrence of the ILF has been predicted for the octahedral product [Pt{CH(CO_2Me)(CN)}$_2$(bipy)(SePh)(Cl)], being the platinum contribution to LUMO + 1 and LUMO + 2 empty σ* molecular orbitals (shown in Figure S3) of 26.4 and 31.1 %, respectively. A similar electronic distribution has been found also in the starting square planar complex [Pt{CH-(CO_2Me)(CN)}$_2$(bipy)]. According to the classic Ligand Field Theory, the d_{x2-y2} orbital in [Pt{CH(CO_2Me)(CN)}$_2$(bipy)] should be empty and largely contribute to the σ* interaction (thus to the LUMO + 3 in the present case, being the LUMO-LUMO + 2 centered on the bipyridine ligand). The d_{x2-y2} calculated contribution to LUMO + 3 is instead lower than 29.0 % while the corresponding bonding orbital is metal centered. Thus, the precursor features a d^{10} configuration, in agreement with a ILF description.

The study of the interaction between [Pt{CH-(CO_2Me)(CN)}$_2$(bipy)] and the PhSe–Cl substrate allows the detection of the intermediate [Pt{CH(CO_2Me)(CN)}$_2$(bipy)]-*PhSe–Cl with a free energy gain of −10.9 kcal mol-1. The optimized geometry of the adduct [Pt{CH(CO_2Me)(CN)}$_2$(bipy)]-*PhSe–Cl is shown in Figure 6 with a quasi linear Pt–Se-Cl arrangement, the angle being 172°. The Se–Cl distance is 0.16 Å elongated compared to the isolated system (2.39 vs. 2.23 Å). The aryl substituent of PhSe–Cl is involved in weak interactions with the bipyridine ligand of the complex. The chloride release provides the cationic intermediate [Pt{CH-(CO_2Me)(CN)}$_2$(bipy)(SePh)]$^+$, shown in Figure 6, with a free energy cost of +19.2 kcal mol^{-1}. The presence of a peripheral carbonyl group in CH(CO_2Me)(CN) ligand allows the formation of an octahedral intermediate rather than a penta-coordinated one with the sixth coordination site occupied by the oxygen. The substitution of the coordinated oxygen with the chloride occurs with a free energy gain as large as −31.7 kcal mol^{-1}.

The analysis of the electronic structure of the [Pt{CH-(CO_2Me)(CN)}$_2$(bipy)(SePh)]$^+$ intermediate revealed the occurrence of the ILF with the metal contribution to the LUMO and LUMO + 1 less than 35 %. The latter contribution is somewhat larger than that found in the final octahedral species [Pt{CH(CO_2Me)(CN)}$_2$(bipy)(SePh)(Cl)] possibly due to the oxygen coordination. To better understand the electronic structure of the cationic intermediate, a simplified model [Pt{CH-(Me)(CN)}$_2$(bipy)(SePh)]$^+$ has been optimized obtaining a square pyramidal intermediate. The resulting LUMO, shown in Figure 7, features a strong contribution from the apical SePh ligand and only 32.4 % from the metal, suggesting once again the ILF occurrence.

The occurrence of the Inverted Ligand Field in all the steps of the reaction allows to conclude that hardly platinum is involved in an oxidative process but more probably it maintains the d^{10} configuration with a somewhat efficient σ back-donation toward the ligands.

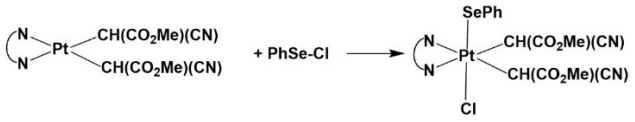

Scheme 3. Study reaction of Se–Cl addition to a square planar platinum complex.

Conclusions

The occurrence of ILF has been shown also for the formal oxidation state IV in octahedral platinum complexes. For the iodide, bromide and chloride, the energy of the d metal orbitals are lower than the "e_g" combination of the ligands and a d^{10} configuration or Pt(0) oxidation state describes better the complexes. Only for the fluoride, a formal oxidation state IV seems to be reasonable. The metal contribution in the antibonding e_g combinations of the halogen complexes is in correlation with the halogen electronegativity.

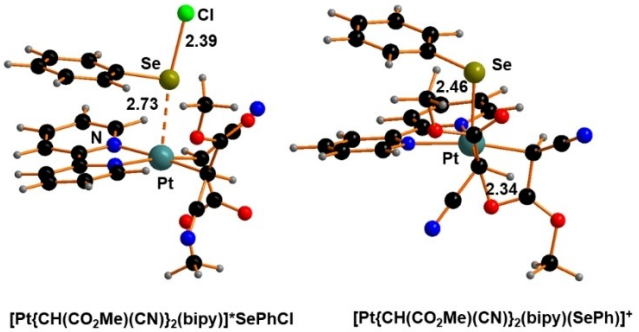

Figure 6. Optimized structure of adduct [Pt{CH(CO_2Me)(CN)}$_2$(bipy)]*SePhCl and cationic species [Pt{CH(CO_2Me)(CN)}$_2$(bipy)(SePh)]$^+$.

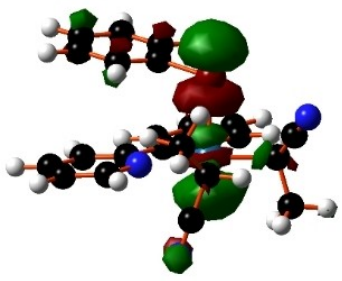

Figure 7. LUMO orbital of the simplified model [Pt{CH-(Me)(CN)}$_2$(bipy)(SePh)]$^+$.

© 2023 The Authors. Chemistry - A European Journal published by Wiley-VCH GmbH

For the elements in the chalcogenide group, the ILF are found for sulfur and selenium complexes as a consequence of a ligand centered antibonding e_g sets. In the case of oxygen, a strong covalent character of the Pt–O bonds has to be invoked, being the antibonding e_g sets occupied at almost 50% for the metal and the ligand.

The oxidative activation of a Se–Cl bond by a square planar Pt(II) complex has been reconsidered in the framework of ILF. Interestingly, in the starting, the final octahedral as well as the intermediate complexes, the Pt metal has a d^{10} configuration and the whole process could be properly classified as not oxidative process.

The obtained results open to the need of new simple and immediate nomenclature rules taking into account a more realistic description of the electronic structure by-passing the classic view of coordination metal-ligand bonding.

Supporting Information

The authors have cited additional references within the Supporting Information (Ref. [48,49]).

Acknowledgements

The computing resources and the related technical support used for this work have been provided by CRESCO/ENEAGRID High Performance Computing infrastructure and its staff.[50] CRESCO/ENEAGRID High Performance Computing infrastructure is funded by ENEA, the Italian National Agency for New Technologies, Energy and Sustainable Economic Development and by Italian and European research programs, see http://www.cresco.enea.it/english for information.

Conflict of Interests

The authors declare no conflict of interest.

Data Availability Statement

The data that support the findings of this study are available in the supplementary material of this article.

Keywords: electronic structure · inverted ligand field · oxidative addition · platinum complexes · solid-state chemistry

[1] R. Hoffmann, S. Alvarez, C. Mealli, A. Falceto, T. J. Cahill, T. Zeng, G. Manca, *Chem. Rev.* **2016**, *116*, 8173–8192.
[2] F. Maseras, K. Morokuma, *Chem. Phys. Lett.* **1992**, *195*, 500–504.
[3] T. A. Albright, J. Burdett, M.-H. Whangbo, *Orbital Interactions in Chemistry*, 2nd ed.; Wiley: Hoboken, NJ, **2013**; p 403.
[4] J. P. Snyder, *Angew. Chem. Int. Ed.* **1995**, *34*, 80–81.
[5] R. C. Walroth, J. T. Lukens, S. N. MacMillan, K. D. Finkelstein, K. M. Lancaster, *J. Am. Chem. Soc.* **2016**, *138*, 1922–1931.
[6] I. M. Dimucci, J. T. Lukens, S. Chatterjee, K. M. Carsch, C. J. Titus, S. J. Lee, D. Nordlund, T. A. Betley, S. N. MacMillan, K. M. Lancaster, *J. Am. Chem. Soc.* **2019**, *141*, 18508–18520.
[7] R. Galassi, L. Luciani, C. Graiff, G. Manca, *Inorg. Chem.* **2022**, *61*, 3527–3539.
[8] D. Joven-Sancho, M. Baya, A. Martín, J. Orduna, B. A. Menjón, *Angew. Chem. Int. Ed.* **2021**, *60*, 26545–26549.
[9] B. L. Geoghegan, Y. Liu, S. Peredkov, S. Dechert, F. Meyer, S. DeBeer, G. E. Cutsail III, *J. Am. Chem. Soc.* **2022**, *144*, 2520–2534.
[10] C. Gao, G. Macetti, J. Overgaardt, *Inorg. Chem.* **2019**, *58*, 2133–2139.
[11] W. Grochala, *J. Supercond. Novel Magn.* **2018**, *31*, 737–752.
[12] G. Manca, F. Fabrizi de Biani, M. Corsini, C. Cesari, C. Femoni, M. C. Iapalucci, S. Zacchini, A. Ienco, *Inorg. Chem.* **2022**, *61*, 3484–3492.
[13] E. A. Trifonova, I. F. Lach, W. B. de Haas, R. W. A. Havenith, M. Tromp, J. E. M. N. Klein, *Angew. Chem. Int. Ed.* **2023**, *62*, e202215523.
[14] A. Perez-Bitrian, S. Alvarez, M. Baya, J. Echeverria, A. Martin, J. Orduna, B. Menjon, *Chem. Eur. J.* **2023**, *29*, e202203181(1–7).
[15] A. Portugués, M. A. Martínez-Nortes, D. Bautista, P. González-Herrero, J. Gil-Rubio, *Inorg. Chem.* **2023**, *62*, 1708–1718.
[16] I. M. DiMucci, C. J. Titus, D. Nordlund, J. R. Bour, E. Chong, D. P. Grigas, C.-H. Hu, M. D. Kosobokov, C. D. Martin, L. M. Mirica, N. Nebra, D. A. Vicic, L. L. Yorks, S. Yruegas, S. N. MacMillan, J. Shearer, K. M. Lancaster, *Chem. Sci.* **2023**,*14*, 6915–6929.
[17] J. A. Aramburu, M. Moreno, *Solid State Commun.* **1986**, *58*, 305–309.
[18] J. A. Aramburu, M. Moreno, *Solid State Commun.* **1987**, *62*, 513–516.
[19] K. Foyevtsova, G. A. Sawatzky, *J. Modern Phys.* **2019**, *10*, 953–965.
[20] M. Oudah, M. Kim, K. S. Rabinovich, K. Foyevtsova, G. McNally, B. Kilic, K. Kuster, R. Green, A. V. Boris, G. Sawatzky, A. P. Schnyder, D. A. Bonn, B. Keimer, H. Takagi, *Phys. Rev. Lett.* **2021**, *5*, 064202(1–9).
[21] W. Grochala, R. G. Egdell, P. P. Edwards, Z. Mazej, B. Zemva, *ChemPhysChem* **2003**, *4*, 997–1001.
[22] E. G. Bowes, S. Pal, J. A. Love, *J. Am. Chem. Soc.* **2015**, *137*, 16004–16007.
[23] R. A. Periana, D. J. Taube, S. Gamble, H. Taube, T. Satoh, H. Fujii, *Science* **1998**, *280*, 560–564.
[24] M. A. Fard, R. J. Puddephatt, *J. Organomet. Chem.* **2020**, *910*, 121139(1–7).
[25] A. Vigalok, *Acc. Chem. Res.* **2015**, *48*, 238–247.
[26] G. Canil, J. Gurruchaga-Pereda, S. Braccini, L. Marchetti, T. Funaioli, F. Marchetti, A. Pratesi, L. Salassa, C. Gabbiani, *Int. J. Mol. Sci.* **2023**, *24*, 1106(1-17).
[27] N. J. Wheate, S. Walker, G. E. Craig, R. Oun, *Dalton Trans.* **2010**, *39*, 8113–8127.
[28] S. Savino, V. Gandin, J. D. Hoeschele, C. Marzano, G. Natile, N. Margiotta, *Dalton Trans.* **2018**, *47*, 7144–7158.
[29] Y. Shi, S.-A. Liu, D. J. Kerwood, J. Goodisman, J. C. Dabrowiak, *J. Inorg. Biochem.* **2012**, *107*, 6–14.
[30] S. Su, Y. Chen, P. Zhang, R. Ma, W. Zhang, J. Liu, T. Li, H. Niu, Y. Cao, B. Hu, J. Gao, H. Sun, D. Fang, J. Wang, P. G. Wang, S. Xie, C. Wang, J. Ma, *Eur. J. Med. Chem.* **2022**, *243*, 114680.
[31] A. Annunziata, A. Amoresano, M. E. Cucciolito, R. Esposito, G. Ferraro, I. Iacobucci, P. Imbimbo, R. Lucignano, M. Melchiorre, M. Monti, C. Scognamiglio, A. Tuzi, D. M. Monti, A. Merlino, F. Ruffo, *Inorg. Chem.* **2020**, *59*, 4002–4014.
[32] T. Yempala, T. Babu, S. Karmakar, A. Nemirovski, M. Ishan, V. Gandin, D. Gibson, *Angew. Chem. Int. Ed.* **2019**, *58*, 18218–18223.
[33] E. Gabano, M. Ravera, I. Zanellato, S. Tinello, A. Gallina, B. Rangone, V. Gandin, C. Marzano, M. G. Bottone, D. Osella, *Dalton Trans.* **2017**, *46*, 14174–14185.
[34] C. R. Groom, I. J. Bruno, M. P. Lightfoot, S. C. Ward, *The Cambridge Structural Database.* **2016**, *72*, 171–179.
[35] A. D. Becke, *Phys. Rev. A* **1988**, *38*, 3098–3100.
[36] E. van Lenthe, A. van der Avoird, P. E. S. Wormer, *J. Chem. Phys.* **1998**, *108*, 4783–4796.
[37] F. Neese, *Wiley Interdiscip. Rev.: Comput. Mol. Sci.* **2022**, *12*, e1606.
[38] L. Pauling, *J. Am. Chem. Soc.* **1932**, *54*, 3570–3582.
[39] M. Rahm, T. Zeng, R. Hoffmann, *J. Am. Chem. Soc.* **2019**, *141*, 342–351.
[40] H. Hillebrecht, G. Thiele, P. Hollmann, W. Preetz, *Z. Naturforsch. B* **1992**, *47*, 1099–1104.
[41] S. Streltsov, V. V. Roizen, A. V. Ushakov, A. R. Oganov, D. I. Khomskii, *Proc. Natl. Acad. Sci. USA* **2018**, *115*, 9945–9950.
[42] J. M. Mc Connachie, M. A. Ansari, J. A. Ibers, *Inorg. Chem.* **1993**, *32*, 3250–3255.
[43] P. S. Cartwright, R. D. Gillard, E. R. J. Sillanpaa, J. Valkonen, *Polyhedron* **1991**, *10*, 2501–2509.

© 2023 The Authors. Chemistry - A European Journal published by Wiley-VCH GmbH

15213765, 2023, 59, Downloaded from https://chemistry-europe.onlinelibrary.wiley.com/doi/10.1002/chem.202301669 by CNR Group, Wiley Online Library on [13/11/2023]. See the Terms and Conditions (https://onlinelibrary.wiley.com/terms-and-conditions) on Wiley Online Library for rules of use; OA articles are governed by the applicable Creative Commons License

[44] I. P. Stolyarov, N. V. Cherkashina, A. V. Churakov, A. V. Naumkin, A. V. Chernyak, V. M. Martynenko, *Russ. J. Inorg. Chem.* **2019**, *64*, 49–55.
[45] X. Chia, A. Ambrosi, P. Lazar, Z. Sofer, J. Luxa, M. Pumera, *Adv. Funct. Mater.* **2016**, *26*, 4306–4318.
[46] D. Dai, H.-J. Koo, M.-H. Whangbo, C. Soulard, X. Rocquefelte, S. Jobic, *J. Solid State Chem.* **2003**, *173*, 114–121.
[47] A. Panunzi, G. Roviello, F. Ruffo, *Inorg. Chem. Commun.* **2003**, *6*, 1282–1286.
[48] Y. Takano, K. N. Houk, *J. Chem. Theory Comput.* **2005**, *1*, 70–77.
[49] R. Dovesi, A. Erba, R. Orlando, C. M. Zicovich-Wilson, B. Civalleri, L. Maschio, M. Rerat, S. Casassa, J. Baima, S. Salustro, B. Kirtman *Wiley Interdiscip. Rev.: Comput. Mol. Sci.* **2018**, *8*, e1360(1–36).
[50] F. Iannone, F. Ambrosino, G. Bracco, M. De Rosa, A. Funel, G. Guarnieri, S. Migliori, F. Palombi, G. Ponti, G. Santomauro, P. Procacci, *International Conference on High Performance Computing & Simulation (HPCS)* **2019**, 1051–1052

Manuscript received: May 25, 2023
Accepted manuscript online: July 31, 2023
Version of record online: September 18, 2023

© 2023 The Authors. Chemistry - A European Journal published by Wiley-VCH GmbH

15213765, 2023, 59, Downloaded from https://chemistry-europe.onlinelibrary.wiley.com/doi/10.1002/chem.202301669 by CNR Group, Wiley Online Library on [13/11/2023]. See the Terms and Conditions (https://onlinelibrary.wiley.com/terms-and-conditions) on Wiley Online Library for rules of use; OA articles are governed by the applicable Creative Commons License